

# Developing a Sky-End Fibre Aperture for the AMASE Fibre Bundle

Goratamang Gaedie  <sup>1,2</sup>, Sabyasachi Chattophadyay<sup>1,2</sup>, and Nidhi Mehandiratta<sup>2,3</sup>

<sup>1</sup> Centre for Space Research, North-West University, Potchefstroom 2520, South Africa

<sup>2</sup> South African Astronomical Observatory, Observatory 7925, Cape Town, South Africa

<sup>3</sup> Department of Astronomy, University of Cape Town, 7700, South Africa

E-mail: [ggaedie@gmail.com](mailto:ggaedie@gmail.com)

**Abstract.** The Affordable Multiple-Aperture Spectroscopy Explorer (AMASE) project aims to enable high-resolution spectroscopy of ionised gas in galaxies. However, fabricating ultradense fibre bundles with micrometre-level precision presents significant challenges. We detail a fabrication process that combines precision machining, stress-reducing handling, and iterative polishing. Although the final prototype did not meet the optical performance targets, our methods reduced manual labour, improved reproducibility, and identified critical failure modes, providing essential information for future astrophotonic instrument designs.

## 1. Introduction

Over the past decade, there has been a growing emphasis on understanding the physical processes governing the interstellar medium (ISM) and star formation in the Milky Way and nearby galaxies [1; 2]. Integral Field Spectroscopy (IFS) has revolutionised this effort, enabling the study of spatially resolved kinematics, ionisation states, and chemical abundances across diverse galactic environments. Surveys such as MaNGA and SAMI have provided crucial insights on kiloparsec scales. However, these surveys lack spatial and spectral resolution to probe the fine structure and turbulence within individual H<sub>II</sub> regions at sub-parsec levels, which is critical to understanding star formation feedback [3; 4].

The Affordable Multiple Aperture Spectroscopy Explorer (AMASE) project addresses this gap through a novel, cost-effective design that combines an array of multifibre spectrographs with telephoto lenses [5]. AMASE targets a spectral resolution of  $R \sim 15,000$  and a spatial resolution ( $\sigma \sim 8.5 \text{ kms}^{-1}$ ) capable of dissecting ionised gas structures from 0.1 to 100 parsecs in the Local Group galaxies. Key science goals of AMASE include: (1) characterising feedback-driven outflows in star-forming regions [6; 3]; (2) disentangling ionisation sources in diffuse ionised gas [3]; (3) calibrating strong-line metallicity diagnostics; and (4) improving photoionisation models with spatially resolved emission line data [4]. Achieving these goals requires precise control over the optical alignment and integrity of the fibre bundles that couple the spectrographs to the sky.

We present the design, fabrication, and metrological validation of the sky-end fibre instrument cable, a key component of the Affordable Multiple-Aperture Spectroscopy Explorer. This system enables high-resolution, integral-field spectroscopy of ionised gas structures in the Milky Way and Local Group galaxies. A high density configuration of 547 fibres within a 1.858 mm regular hexagonal aperture achieves a core area-to-hexagon area ratio of approximately 50%, maximising

photon throughput. We report on the design, metrology, and analysis of the quality of the fibre bundle.

Section 2 details the fabrication methodology; Section 3 summarises the optical and mechanical test results; Section 4 discusses limitations and future improvements; and Section 5 concludes.

## 2. Fabrication Methodology

The AMASE instrument uses 547 fibres with a core diameter of 50  $\mu\text{m}$ , each providing a spatial resolution of approximately 25.24 arcseconds on-sky. These fibres cover a hexagonal on-sky footprint with a long-axis span of 19.3 arcminutes, equivalent to a total field of view of roughly 79  $\text{arcmin}^2$  per spectrograph. The fibres are arranged in a hexagonal close-packed (HCP) geometry to maximise the fill factor and minimise interstitial space.

The nominal aperture dimension from corner to corner is 1.894 mm. However, practical assembly constraints necessitated additional clearance to account for fibre-dimensional variability. The clearance was defined as follows:

$$\text{Clearance} = \Delta d \times \sqrt{N} \quad (1)$$

where  $\Delta d$  is the tolerance for the diameter of the fibre and  $N$  is the number of fibres along the dimension. Given (from the fibre supplier) a typical fibre diameter tolerance of  $\pm 1 \mu\text{m}$ , the required clearance becomes:

$$\text{Clearance} = 1 \mu\text{m} \times \sqrt{27} \approx 5.20 \mu\text{m} \quad (2)$$

The aperture diameters were then evaluated as offsets above the nominal value in multiples of the clearance. Extensive empirical testing identified that aperture dimensions should be in the range:

$$\text{Aperture} = 1.894 \text{ mm} + m \times \text{Clearance} \quad (3)$$

where  $m$  is a multiple of our clearance factor. We made six different apertures of clearance sized (1.894 mm, 1.905 mm, 1.917 mm, and 1.928 mm) in addition to the nominal aperture size. All apertures were machined with entry and exit chamfers to minimise surface-edge interference and aid fibre guidance.

Figure 1 shows the measurement of the smallest circle that fits within an aperture corner, used for quality assessment. These inspections were critical to verifying the dimensional conformity and suitability of the fabricated apertures.

### 2.1. Fibre Handling and Insertion

For each attempt to insert into an aperture, we cut 547 fibres of the same size. [7; 8] mentions that stress on the fibres can lead to focal ratio degradation (FRD). Therefore, employing a cleaver is crucial as it minimises stress or potential damage to the fibres and reduces the roughness of the terminated surface.

We used a packing jig to push the fibres into the aperture and also attempted a manual insertion. Large fibres with strong core diameters (such as SMI 200 (200  $\mu\text{m}$  core [9])) can be inserted by collectively pushing the bundle through a precision machined aperture, an approach that fails for weaker fibres 50  $\mu\text{m}$  (core diameter) that tend to buckle.

Our first attempt was to insert the fibres into the nominal aperture size of 1.894 mm we strip the fibre buffer. We used 98% sulphuric acid, heated it to a temperature of 180  $^{\circ}\text{C}$ . The dipped length of the fibres was perturbed to accelerate the reaction. The safety procedure for handling acid can be found in Reflecta Laboratory Supplies material safety data sheet (MSDS). After

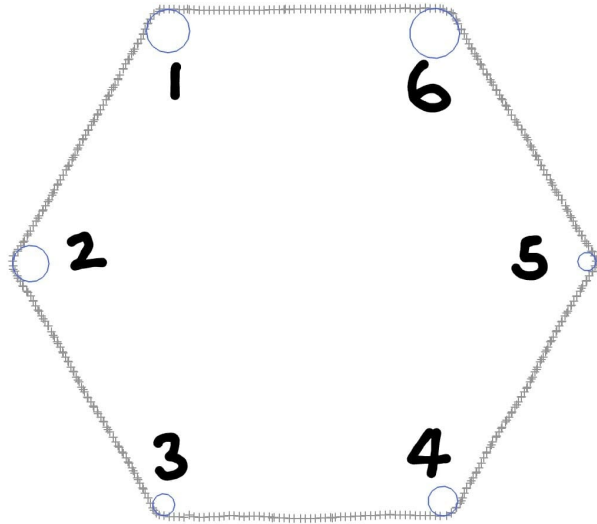


Figure 1: Microscopic (shadowgraph) inspection of the aperture quality and dimensional conformity. At each corner of the hexagonal aperture, the smallest possible circle has been fitted. The radii of these circles are: (1) 0.081 mm, (2) 0.068 mm, (3) 0.042 mm, (4) 0.056 mm, (5) 0.035 mm, and (6) 0.094 mm.

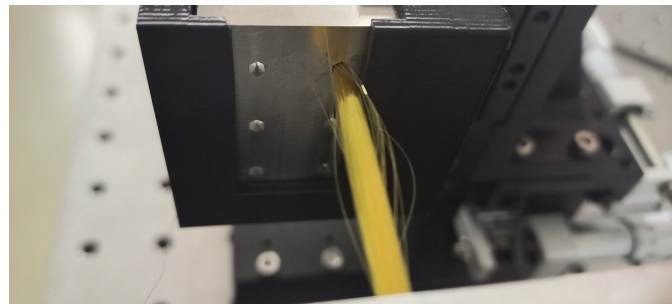


Figure 2: Packing jig and aperture holder used for staged fibre insertion.

stripping the fibres, we dipped them in deionised water to neutralise the chemical reaction. The buffer-stripped fibres were bundled together using a heat shrink tube. We tried to push the stripped part of the fibres through the aperture followed by the unstripped part. The stripped part of the fibres easily broke, and the aperture was too tight to push the unstripped part of the fibre bundle into it.

Finally, we used isopropyl alcohol (IPA) to keep the fibres together, preventing them from spreading. We insert the fibres inside an IPA bath and inside an ultrasonic cleaner. We eased the insertion a bit by thermally expanding the aperture. We were able to effectively push all the fibres by immersing them in IPA and threading them through the 1.931 mm aperture after raising both the room and aperture temperatures. The aperture of 1.931 mm proved to be the smallest feasible one that we could employ.

### 2.2. Adhesive Application and Curing

To ensure that the fibres remain intact and placed within, we use a transparent two-part epoxy adhesive 301 2.5GM BI-PAK 80168250001 from Epoxy Technology, Inc (EPO-TEK); the epoxy components are mixed within their original packaging prior to opening. After mixing, the two-part epoxy glue is poured into a resealable plastic cup. We carefully used a gauge 18 needle

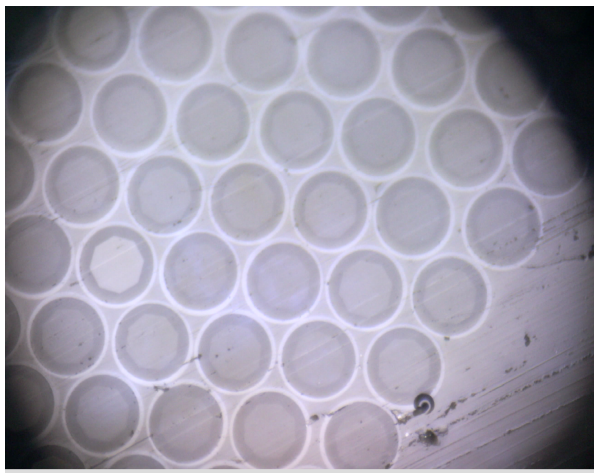
syringe to draw the glue from the cup, minimising the introduction of air bubbles. The glue is applied in phases to the fibre bundle; initially, it is added to the fibres on the aperture's exit side, allowing it to penetrate by gently separating the fibres. The bundle is then slightly retracted through the aperture to facilitate glue flow. The bundle is left undisturbed at room temperature for 48 hours to fully cure. The result is depicted in Figure 3.



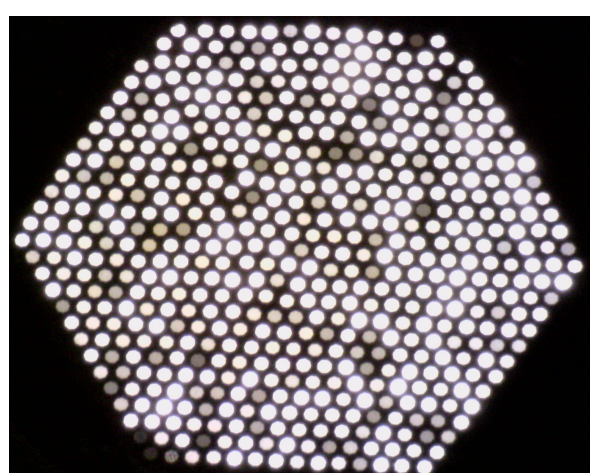
Figure 3: Fibre bundle after epoxy curing.

### 2.3. Polishing and Surface Preparation

The fibre bundle was subjected to a thorough multistep polishing process using various micron-scale polishing disks, as described by [10]. Initially, the fibre bundle was subjected to rough polishing, followed by a sequence with disks of 30, 15, 5, 3 and 1  $\mu\text{m}$  (2 hours each at 5, 5,4,5,3,5, and 1 rotation per second, respectively). Adjustments were made in vertical load, speed and angle to correct surface imperfections such as uneven patches and scratches. These irregularities were traced back to the polishing setup, not the fibre bundle. This iterative process with each disk finally achieved a smooth, polished surface, as shown in Figure 4a. Figure 4b shows the fully polished bundle.



(a) Final 1  $\mu\text{m}$  polish showing scratch-free end faces.



(b) Completed fibre bundle after polishing and inspection.

Figure 4: Polishing and inspection results.

### 3. Results

The measurement and analysis in error of the accuracy of the positioning of the fibres along the x and y axes, respectively, were performed as detailed by Gaedie et al. [11]. Fibre centroids were extracted from high-resolution microscope images using a custom Python-based image processing pipeline that applied thresholding, morphological filtering, and ellipse fitting. These detected positions were compared with an ideal hexagonal grid or an adaptively generated irregular grid, allowing for precise quantification of fibre placement deviations.

For the AMASE-SAAO fibre bundle, positional error analysis yielded standard deviations of  $\sigma_x = 14.79 \mu\text{m}$  and  $\sigma_y = 11.10 \mu\text{m}$ , with a radial error of  $\sigma_r = 9.50 \mu\text{m}$ . These deviations reflect the practical limitations of packing 50  $\mu\text{m}$  core fibres with low bending stiffness into a confined geometry, highlighting the importance of precise aperture machining and insertion techniques to minimise fibre misalignment.

### 4. Discussion

This project aimed to produce and evaluate a high-density fibre bundle for the AMASE spectrograph. Despite numerous efforts and extensive design revisions, the project did not meet its anticipated performance criteria, largely due to difficulties with accurately inserting fibres into apertures with precise tolerances. One key issue was inserting fibres into apertures that were either too tight or inadequately fitted. The required extremely fine tolerances further complicated the process. Redesigns involved enlarging aperture hole sizes, experimenting with different fibre types such as serum optical polymicro fibres, and trying varied insertion techniques, including chemical stripping and ultrasonic cleaning. However, achieving successful insertion with sufficient positional accuracy remained elusive. Even when fibres were successfully inserted, as in a 1.931 mm aperture, inconsistencies in the packing, ranging from 20 to 25  $\mu\text{m}$ , greatly exceeded the precision  $\pm 3 \mu\text{m}$  required for astronomical use. The uneven internal walls of the apertures further complicated the insertion process, and although polishing somewhat improved the situation, issues such as poor fill factors and uneven bundle faces persisted. A significant finding was related to the handling of fibres with varying diameters. For example, sturdier fibres, such as those in the SMI-200 bundle (240  $\mu\text{m}$  in diameter with buffer), were easier to insert without bending due to their rigidity. Their structural strength and easier creation of smooth inner walls for larger holes facilitated a straightforward assembly process. In contrast, the smaller diameter fibres used in the AMASE bundles (79  $\mu\text{m}$ ) posed considerable challenges during fabrication and assembly, being more susceptible to bending and damage during insertion.

### 5. Conclusion

The development of a fibre instrumentation cable for AMASE was ultimately unsuccessful, despite improving our understanding of the physical and mechanical limits of the fibre bundle assembly; the project did not meet the required optical and positional criteria. The key conclusions are as follows.

- Injection of fibres into tight apertures with micrometre-level tolerance proved ineffective because of their mechanical fragility and size inconsistencies.
- The packing precision did not meet the standard  $\pm 3 \mu\text{m}$ , with deviations often exceeding 20  $\mu\text{m}$ .
- The polishing and termination processes added variability, which affected the uniformity of the fibre face.

These results reveal that conventional manual fabrication methods are not adequate for producing ultradense, small-core fibre bundles with high precision. Future work should investigate the following,

- Employ laser micro-machining or precision machining techniques for aperture fabrication.
- Adopt alternative designs such as individually machined fibre holes to prevent collective misalignment.
- Using alignment jigs and automated insertion tools to improve repeatability.
- Enhancing adhesive application techniques to ensure consistent distribution and reduce stress.

Although the project did not deliver the intended instrument, it has provided essential insight into the current limitations of fibre bundle fabrication methods. These findings will inform the next development phase for AMASE or similar astrophotonic instrumentation projects.

## References

- [1] Kennicutt R C and Evans N J 2012 *ARA&A* **50** 531–608 (*Preprint* 1204.3552)
- [2] Ferrière K M 2001 *Reviews of Modern Physics* **73** 1031–1066 (*Preprint* astro-ph/0106359)
- [3] Zhou L, Federrath C, Yuan T, Bian F, Medling A M, Shi Y, Bland-Hawthorn J, Bryant J J, Brough S, Catinella B, Croom S M, Goodwin M, Goldstein G, Green A W, Konstantopoulos I S, Lawrence J S, Owers M S, Richards S N and Sanchez S F 2017 *MNRAS* **470** 4573–4582 (*Preprint* 1706.04754)
- [4] Oh S, Colless M, D’Eugenio F, Croom S M, Cortese L, Groves B, Kewley L J, van de Sande J, Zovaro H, Varidel M R, Barsanti S, Bland-Hawthorn J, Brough S, Bryant J J, Casura S, Lawrence J S, Lorente N P F, Medling A M, Owers M S and Yi S K 2022 *MNRAS* **512** 1765–1780 (*Preprint* 2202.10469)
- [5] Yan R, Bershady M A, Smith M P, MacDonald N, Bizyaev D, Bundy K, Chattopadhyay S, Gunn J E, Westfall K B and Wolf M J 2020 *Ground-based and Airborne Instrumentation for Astronomy VIII (Society of Photo-Optical Instrumentation Engineers (SPIE) Conference Series* vol 11447) ed Evans C J, Bryant J J and Motohara K p 114478Y (*Preprint* 2105.11471)
- [6] Law D R, Belfiore F, Bershady M A, Cappellari M, Drory N, Masters K L, Westfall K B, Bizyaev D, Bundy K, Pan K and Yan R 2022 *The Astrophysical Journal* **928** 58 URL <https://dx.doi.org/10.3847/1538-4357/ac5620>
- [7] Allington-Smith J, Dunlop C, Lemke U and Murray G 2013 *Monthly Notices of the Royal Astronomical Society* **436** 3492–3499 ISSN 0035-8711 (*Preprint* <https://academic.oup.com/mnras/article-pdf/436/4/3492/3110747/stt1842.pdf>) URL <https://doi.org/10.1093/mnras/stt1842>
- [8] Eigenbrot A D, Bershady M A and Wood C M 2012 *Ground-based and Airborne Instrumentation for Astronomy IV* vol 8446 (SPIE) pp 1822–1831 URL <https://scholar.google.com/scholar?q=Eigenbrot+A.+D.%2C+Bershady+M.+A.+and+Wood+C.+M.+2012+Proc.+SPIE+8446+84465W>
- [9] Chattopadhyay S and Bershady M A 2024 *Ground-based and Airborne Instrumentation for Astronomy X* vol 13096 ed Bryant J J, Motohara K and Vernet J R D International Society for Optics and Photonics (SPIE) p 130962R URL <https://doi.org/10.1117/12.3017822>
- [10] Smith M P, Chattopadhyay S, Hauser A, Oppor J E, Bershady M A and Wolf M J 2020 *Advances in Optical and Mechanical Technologies for Telescopes and Instrumentation IV* vol 11451 ed Navarro R and Geyl R International Society for Optics and Photonics (SPIE) p 114516W URL <https://doi.org/10.1117/12.2563201>
- [11] Gaedie G A, Chattopadhyay S, Mehandiratta N, Yan R, Hui S C H, Lin Z, Qiao Y, Ho I S W, Zhu A Y, Cheung D Y H, Lee M Y L, Zhang J, Zhou R, Lam Y C, Chen Q and Wang Y 2025 *Proceedings of SPIE – Ground-based and Airborne Instrumentation for Astronomy X* (International Society for Optics and Photonics)

## APPENDIX A: CAD drawing for the 1.931 mm aperture

